Polymer Chemistry

ROYAL SOCIETY OF CHEMISTRY

PAPER

View Article Online
View Journal | View Issue

Cite this: *Polym. Chem.*, 2024, **15**, 1347

Vanillin-based dual dynamic epoxy building block: a promising accelerator for disulfide vitrimers†

Solène Guggari,[a,b] Fiona Magliozzi,[b] Samuel Malburet,[b] Alain Graillot,[b] Mathias Destarac[a] and Marc Guerre*[a]

Epoxies are one of the most versatile thermoset materials owing to their outstanding physical and chemical properties. In recent years, there have been concerted efforts to enhance the sustainability and durability of epoxy materials across a wide range of industrial applications. In this regard, vitrimers, a class of polymeric materials combining the advantages of thermosets and the recyclability of thermoplastics, have attracted significant attention. The combination of two or more covalent or non-covalent dynamic chemistries holds great promise for introducing accelerated yet tailored dynamic exchanges. Therein, a dual-dynamic bio-based epoxy building block containing both imine and disulfide bonds (DDBB), synthesized from cystamine and vanillin, has been compared to its imine-containing single dynamic analogue (SDBB). A substantial acceleration of dynamic exchanges (reflected by a decrease of the relaxation time from 4 min to 3 s at 160 °C) was revealed owing to simultaneous exchanges of imine and disulfide moieties. Building upon this, this dual-dynamic epoxy building block was introduced as a doping agent in disulfide vitrimer formulations to accelerate the dynamic bond exchanges. The results demonstrated a remarkable enhancement in exchange rates, with the relaxation time at 190 °C decreasing to as low as 21 s (with 30 w/w% of DDBB), as opposed to 25 min for the undoped counterpart. This enhancement was accomplished with minimal impact on the glass transition temperature and without substantial alteration of the curing behaviour.

Received 11th January 2024,
Accepted 26th February 2024

DOI: 10.1039/d4py00038b

rsc.li/polymers

Introduction

Owing to their three-dimensional structure and their chemical resistance, epoxy thermosets are the materials of choice for numerous applications, encompassing coatings, adhesives and composite materials.[1,2] However, as a result of their permanently crosslinked networks, thermosets cannot be reprocessed or reshaped after curing and are usually destined for landfill disposal or incineration. Therefore, the development of recyclable epoxy thermosets exhibiting high mechanical performance, yet with reprocessability and reparability, recently attracted considerable attention.[3–8]

In this context, a new class of dynamic crosslinked materials, coined vitrimers, has emerged as a sustainable alternative.[9–12] Because of their unique structure, they can reversibly rearrange their network topology with temperature combining both the benefits of thermoplastics, which can be easily reprocessed, with the mechanical resilience of thermosets.[10] Among the various dynamic chemical reactions implemented or purposely developed, disulfide exchanges have gained particular interest.[11,13–15] Luzuriaga *et al.*[13] popularized this chemistry through the use of 4-aminophenyl disulfide (4AFD) that can be readily introduced as a dynamic hardener into epoxy resin formulations. However, the reprocessing of these materials often requires extended time or relatively elevated temperature. The reduction of reprocessing time and temperature is a subject of attention as this chemistry has shown some limitations at high temperature.[16,17] In the course of developing disulfide vitrimers with faster stress relaxation, researchers have explored the possibility to combine several dynamic chemistries within the same material. For example, accelerating effects were reported by employing disulfide exchanges in combination with transesterification.[18–20] Interestingly, both exchange chemistries seemed to facilitate faster reprocessing. Additionally, Dichtel and co-workers[21] observed that the introduction of disulfide exchanges into polyhydroxyurethane networks led to a swifter reprocessing. Regarding epoxies, Xiang *et al.*[22] reported the use of two dis-

[a]*Laboratoire Softmat, Université de Toulouse, CNRS UMR 5623, Université Paul Sabatier, 118 route de Narbonne, 31062 Toulouse Cedex 9, France. E-mail: marc.guerre@cnrs.fr*
[b]*SPECIFIC POLYMERS, Zac Via Domitia, 150 Avenue des Cocardières, 34160 Castries, France*

† Electronic supplementary information (ESI) available. See DOI: https://doi.org/10.1039/d4py00038b

tinct curing agents, each featuring different dynamic bonds: one with aromatic disulfide bonds and the other with aromatic imine bonds. This combination led to the formation of dual dynamic crosslinks, yielding both homogeneous and faster-relaxing epoxy networks. Recently, efforts were made to introduce both exchangeable moieties within the same building block in order to prevent multimodal reactivities. Luo *et al.*[23] synthesized an asymmetrical curing agent composed of phenol and amine functionalities. This curing agent was prepared *via* Schiff base reaction between amine from 4AFD and aldehyde from vanillin and then used as such as a hardener with Bisphenol A diglycidyl ether (DGEBA). They subsequently crosslinked this building block at elevated temperatures through a mechanism that was not clarified. Xu *et al.*[24] reported the synthesis of a symmetrical bis-epoxy building block containing both disulfide and imine functionalities, obtained by combining 4AFD and *p*-hydroxybenzaldehyde followed by epoxidation. Later, a similar strategy was reported in which the hydroxybenzaldehyde was replaced by vanillin for the preparation of a bis-epoxy building block.[25] Therein, our approach shares similarities with the reported methods, yet it is differentiated by two distinctive enhancements: (1) the substitution of the petro-based 4AFD with a bio-based alternative, and (2) the design of symmetrical functionalities to prevent multimodal reactivity.

In this study, we report the synthesis of a partially bio-sourced symmetrical epoxy building block derived from vanillin and cystamine. After crosslinking with DETDA, its dynamic properties were carefully compared to disulfide-free imine-based epoxy analogue. Then, this epoxy was regarded as a potential accelerating agent for enhancing disulfide-based vitrimer exchanges in DGEBA/4AFD formulations. Indeed, in our previous work, an aliphatic disulfide hardener (*i.e.* cystamine) has shown an unexpected accelerating effect on disulfide dynamic exchanges with only 2 to 20% of molar fraction of cystamine added to the aromatic disulfide formulation.[26] However, the reactivity of aromatic and aliphatic amines with epoxies was significantly different. This resulted in bimodal reactivity which could potentially hinder the further development of this formulation for composite manufacturing. Therefore, with this new partially bio-based building block, the suppression of bimodal reactivity is thus expected, preferably without substantial alteration of the curing behaviour and glass transition.

Experimental

Materials

4-Aminophenyl disulfide hardener (4AFD, 98%, AHEW (amine hydrogen equivalent weight) = 62.09 g per eq), hexamethylenediamine, *N,N*-dimethylformamide (DMF), dimethyl sulfoxide (DMSO), tetrahydrofuran (THF), chloroform ($CHCl_3$) and dichloromethane (DCM) were purchased from Sigma Aldrich and used as received. Monogycidyl ether of vanillin (MGEV, SP-9S-5-008) and cystamine (SP-2-4-001) were produced by Specific Polymers and used for the production of SDBB and DDBB derivatives. Diglycidyl ether of bisphenol A (DGEBA, EEW (Epoxy equivalent weight) = 178.9 g per eq), diethyltoluenediamine (DETDA) and vanillin were provided by Specific Polymers.

Synthetic procedures

Synthesis of single-dynamic (SDBB) and dual-dynamic building block (DDBB)

General procedure. MGEV (10 g, 1 eq.) was dissolved in 100 ml of dichloromethane and placed in a 250 ml round bottom flask containing molecular sieves. Then hexamethylenediamine (0.5 eq.) was added and the reacting medium was let at room temperature, under magnetic stirring. After 6 hours, the medium was filtrated in order to withdraw the molecular sieves and washed 3 times with water, dried over Na_2SO_4 and concentrated under vacuum. To remove residual traces of MGEV, the product was triturated in ether. The final precipitated product was recovered as a white powder and dried under vacuum (yield: 84%, epoxy content: 3.5 meq per g, EEW = 285.7, 93% purity, 96% functionality).

^{1}H NMR (300 MHz, $CDCl_3$ Fig. 2a) δ (ppm) = 1.14 (4H, s, C$\underline{H}_2$–CH_2–CH_2–N=C), 1.70 (4H, s, CH_2–C$\underline{H}_2$–CH_2–N=C), 2.76 (2H, m, CH_2 oxirane ring), 2.91 (2H, m, CH oxirane ring), 3.39 (2H, m, oxirane ring), 3.58 (4H, m, CH_2–CH_2–C$\underline{H}_2$–N=C), 3.93 (6H, s, CH_3), 4.08 (2H, dd, C$\underline{H}_2$–C_2H_3O), 4.26 (2H, dd, C$\underline{H}_2$–C_2H_3O), 6.91–6.94 (2H, dd, C$\underline{H}$ aryl), 7.09–7.12 (2H, dd, C$\underline{H}$ aryl), 7.41 (2H, d, C$\underline{H}$ aryl), 8.16 (2H, s, CH–CH_2–CH_2–CH_2–N=C–$\underline{H}$).

Alternatively, DDBB was synthetized according to the same general procedure but using cystamine instead of hexamethylenediamine. The final product was recovered as a white powder (yield: 43%, epoxy content: 3.25 meq per g, EEW = 307.7, 85% purity, 94% functionality).

^{1}H NMR (300 MHz, acetone-d6, Fig. 2b) δ (ppm) = 2.71–2.74 (2H, dd, C$\underline{H}_2$ oxirane ring), 2.82–2.84 (2H, dd, C$\underline{H}_2$ oxirane ring), 3.33 (2H, m, CH oxirane ring), 3.08 (4H, m, CH_2–C$\underline{H}_2$–S–S), 3.86 (6H, s, CH_3), 3.89 (4H, m, C$\underline{H}_2$–CH_2–S–S), 3.8 (2H, dd, C$\underline{H}_2$–C_2H_3O), 4.4 (2H, dd, C$\underline{H}_2$–C_2H_3O), 6.99–7.01 (2H, dd, C$\underline{H}$ aryl), 7.20–7.23 (2H, dd, CH aryl), 7.45 (2H, d, CH aryl) 8.26 (2H, s, CH_2–N=C–$\underline{H}$).

Synthesis of phenolic dual-dynamic building block (ph-DDBB). Vanillin (10 g, 1 eq.) was dissolved in 100 ml of dichloromethane and placed in a 250 ml round bottom flask, together with 5 g (0.5 eq.) of cystamine. The reacting mixture was heated up to reflux and let under magnetic stirring for 24 hours. At the end of the reaction, the organic phase was washed, dried over Na_2SO_4 and dried under vacuum. The ph-DDBB was then recovered as a yellow powder (85.4% purity).

^{1}H NMR (300 MHz, DMSO-d6) δ (ppm) = 9.49 (2H, s large, O$\underline{H}$), 8.2 (2H, s, S–CH_2–CH_2–N=C–$\underline{H}$), 7.31 (2H, s, aryl), 7.11 (2H, d, aryl), 6.81 (2H, d, aryl), 3.78 (6 + 4H, m, O–C$\underline{H}_3$ + S–CH_2–C$\underline{H}_2$–N=C–H) 3.04 (4H, t, S–C$\underline{H}_2$–CH_2–N=C–H).

Preparation of dynamic epoxy resins DDBB/DETDA and SDBB/DETDA

DDBB and SDBB-based epoxy vitrimers were formulated according to eqn (1) and (2) with the molar ratio of the epoxy groups to amine functions fixed at 1 : 1:

$$\text{AHEW} = \frac{\text{Molecular weight of hardener}}{\text{Number of active H}} \quad (1)$$

$$\text{phr} = \frac{\text{AHEW}}{\text{EEW}} \times 100 \quad (2)$$

with (EEW) epoxide equivalent weight, (AHEW) amine hydrogen equivalent weight and phr (per hundred resin) the quantity of amine hardener required to cure 100 g of epoxy resin. According to (1), the AHEW of the DETDA was calculated at 44.57 g per eq. phr for SDBB and DDBB were 15.60 g and 14.48 g, respectively.

Synthetic procedure. As a typical procedure, the DDBB/DETDA vitrimer was prepared by the reaction of DDBB with DETDA. Firstly, DDBB was melted at 90 °C for 30 min to afford viscous state, then DETDA was added and the DDBB/DETDA mixture was stirred and mixed homogeneously at 90 °C for 5 min. Afterward, the mixture was cured as follows: 90 °C for 1 h, 150 °C for 2 h, and 170 °C for 3 h to obtain a fully cured material. SDBB/DETDA was synthesized following the same protocol.

Preparation of DGEBA/DDBB epoxy vitrimers with 4AFD. EEW of DGEBA/DDBB mixtures was calculated according to eqn (3):

$$\text{EEW of mix} = \frac{\text{Total weight}}{\frac{\text{Weight of A}}{\text{EEW of A}} + \frac{\text{Weight of B}}{\text{EEW of B}}} \quad (3)$$

Then the amount of hardener needed for 100 g of epoxy resin was easily calculated from the epoxide equivalent weight of DDBB/DGEBA (EEW of mix) and AHEW, according to eqn (4). Following previous works,[27] an excess of hardener is recommended to exhibit fast enough dynamic exchanges in disulfide-based vitrimer formulations. Hence, 1.2 equivalent of curing agent was introduced in all 4AFD-based formulations.

$$\text{phr} = \frac{1.2 \times \text{AHEW}}{\text{EEW of mix}} \times 100 \quad (4)$$

AHEW of the 4AFD was calculated to 62.09 g per eq.

Synthetic procedure. DDBB was added in different weight ratios (0, 10, 20 and 30 w/w%) to DGEBA/4AFD formulations in order to accelerate dynamic exchanges. In a typical procedure (70% DGEBA/30% DDBB), the epoxy resin (DGEBA, 0.7 g) was first melted at 100 °C for 10 min. Then, 0.3 g of DDBB and 0.364 g of the diamine hardener 4AFD were added. The mixture was stirred mechanically for 5 min at room temperature to afford a homogeneous viscous liquid. The mixture was then cured at 110 °C for 1 h then 2 h at 150 °C for 2 h and 170 °C for 3 h.

Methods and characterizations

Nuclear Magnetic Resonance (NMR) ^{1}H NMR spectrum were recorded on a Bruker Avance 300 (300 MHz) spectrometer equipped with a QNP probe at room temperature. Acetone-d6, DMSO-d6 or methanol-d4 were used as deuterated solvent. Chemical shifts (δ) are given in ppm referenced to the residual deuterated solvent peak.

The epoxide index (EI, meq per g) was determined according to ^{1}H NMR titration method (^{1}H qNMR). The method consists in solubilizing a known mass of the product and external standard (trioxane with a purity of 99.9%). The number of moles of epoxide per gram of product was measured by comparing the standardized integration of the standard with the standardized integration of the oxirane rings.

The epoxy equivalent weight (EEW, g per eq) was determined thanks to the EI (meq per g) using the following eqn (5):

$$\text{EEW} = 1000/\text{EI} \quad (5)$$

Differential scanning calorimetry (DSC) was conducted on a Mettler Toledo Differential Scanning Calorimeter under a constant nitrogen flow rate (50 ml min^{-1}). The samples of about 3–6 mg were heated from 20 °C to 250 °C at the rate of 10 °C min^{-1} under nitrogen. Then, the glass transition temperature was measured in the second heating cycle from 20 °C to 250 °C at the rate of 10 °C min^{-1} under nitrogen and no residual curing heat was observed.

Thermogravimetric analysis (TGA) was performed on a DuPont Instruments 951 Thermal Analyzer (USA) using 8–10 mg of the cured sample. Samples were heated under a nitrogen atmosphere (N_2) at a constant ramp rate of 10 °C min^{-1} from room temperature to 800 °C.

Fourier transform infrared spectroscopy (FTIR) was recorded on a Thermo Nicolet NEXUS spectrophotometer equipped with an ATR diamond. All samples were analyzed through 16 scans and within a range of 400–4000 cm^{-1} for both cured and uncured states.

Stress relaxation experiments. These characterizations were carried out using a 8 mm plate-plate geometry on epoxy resin samples with thicknesses of 0.8–0.4 mm. Prior to the experiments, it was checked that 1% deformation was within the linear viscoelastic region range using strain sweep experiments at 170 °C. A 1% strain was applied for all samples at temperatures ranging from 120 to 200 °C with constant normal force of 5 N. The materials were reprocessed on a lab press instrument (Carver Model C laboratory press) at 170 °C under 0.01 MPa for 35 to 60 min.

Results and discussion

Synthesis and characterization of single and dual dynamic building blocks

Vanillin (Fig. 1), obtained from the alkaline oxidation of lignin, is one of the most used bio-based compound for the preparation of sustainable thermosets.[28–31] Its aldehyde and phenolic functions can be readily functionalized *via* diverse modification techniques, and its aromatic structure imparts high thermal and mechanical properties to the materials. Therein, vanillin was used to synthesize two original symmetrical epoxy building blocks (Fig. 1).

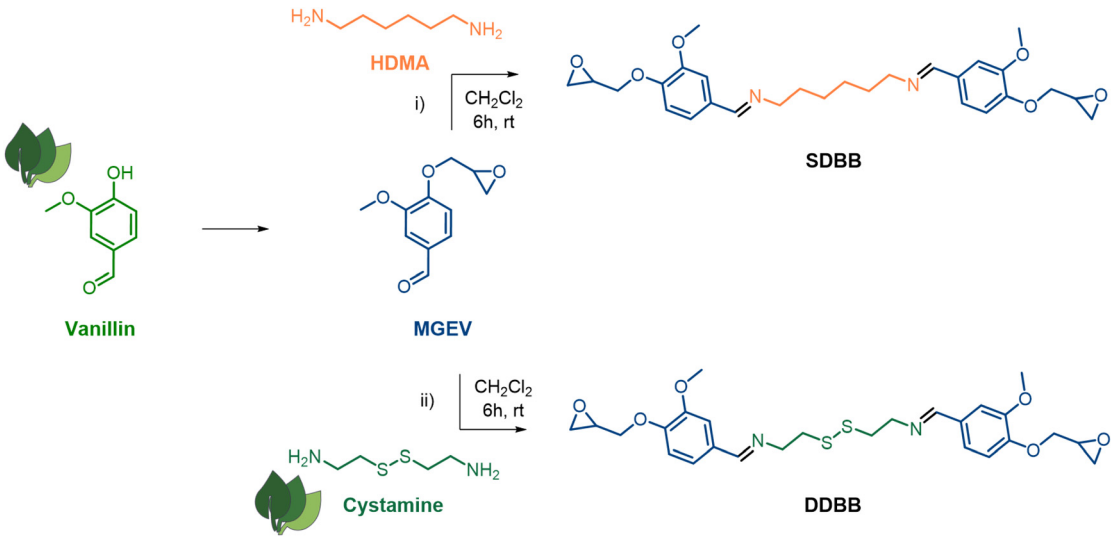

Fig. 1 Synthetic routes for the synthesis of single imine-based epoxy building block (i, SDBB) and dual imine/disulfide-based epoxy building block (ii, DDBB).

First, the imine-based building block (SDBB, Fig. 1, i) was prepared from MGEV (epoxidized vanillin) and hexamethylene-1,6-diamine (HMDA) *via* a Schiff base condensation reaction. Following a similar procedure, a dual-dynamic building block, called DDBB, was also synthesized but this time with cystamine, issued from an amino acid. This resulted in bis-epoxy building block with both imine and disulfide functions (DDBB, Fig. 1, ii). Both epoxy compounds were obtained as a white powder, after 6 hours of reaction at room temperature. After a classical workup procedure, their chemical structure was verified by ^{1}H NMR (Fig. 2).

Fig. 2 illustrates the complete assignment of ^{1}H NMR spectra of DDBB and SDBB. The formation of the targeted structures is evidenced by the presence of imine bond signals at approximately 8.2 ppm in both SDBB and DDBB building blocks. The incorporation of the disulfide bond into DDBB structure is corroborated by distinctive signals at 3.08 and 3.89 ppm, corresponding to the alpha and beta positions of the disulfide bond. In contrast, SDBB exhibits a chemical shift of 1.5 ppm for aliphatic protons.

Notably, both reactants display quantitative (Fig. S1 and S2†) characteristic CH_2 epoxy signals within the range of 2.5–3.0 ppm. To account for the potential occurrence of a small fraction of epoxy opening during the synthesis and ensure accurate stoichiometry, we determined the Epoxide Index (EI, meq per g) using the ^{1}H NMR titration method for both building blocks. The epoxy content for SDBB was found to be 3.5 meq per g, while for DDBB, it was measured at 3.25 meq per g.

Besides, FTIR and DSC analyses were performed on both SDBB and DDBB powders. Respective melting points were 127 °C and 67 °C (see Fig. S3–S6†).

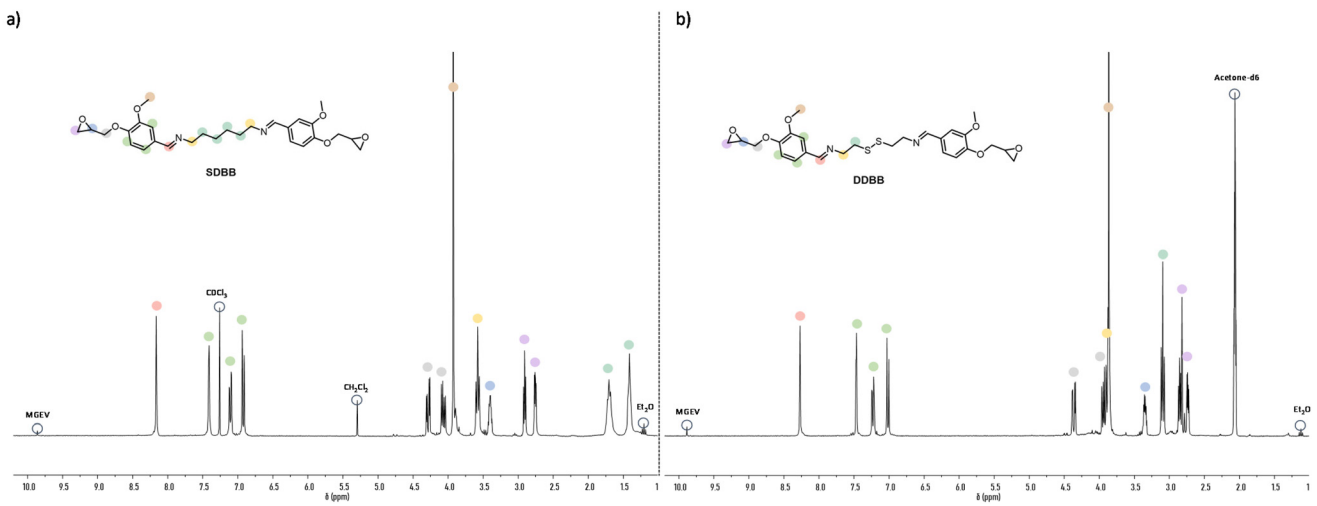

Fig. 2 ^{1}H NMR spectra of (a) SDBB in $CDCl_3$ and (b) DDBB in acetone-d6 at 25 °C.

Preparation of epoxy vitrimers and evaluation of dynamic properties

Epoxy vitrimers were prepared following the conditions depicted in Fig. 3 from the above-synthesized building blocks SDBB and DDBB, and a commonly used diamine hardener DETDA.

The hardener DETDA reacted with epoxy functions to form tertiary amines and hydroxyl groups with embedded functions that can promote dynamic exchanges through Schiff base (imine) exchange for SDBB and thiol-disulfide/imine exchanges[32] for DDBB. The crosslinking process was carried out without the use of solvents and did not release any volatile compounds, which is a crucial requirement to prevent the formation of porosity. However, both DDBB and SDBB exhibited a relatively high melting point (127 °C and 67 °C for SDBB and DDBB, respectively) making impossible the formulation of homogeneous mixtures at ambient temperature. For this reason, the formulations were all conducted at 90 °C in order to perform a comparable formulation process. This temperature has been chosen as a compromise between achieving homogeneous formulations and minimizing the risks associated with crosslinking (see DSC thermograms in Fig. S7†). Because of the relatively high viscosity even at 90 °C for both building blocks, there are still ongoing challenges in formulating this resin for meeting the requirements of conventional industrial processing (for a potential solution, see the section with DGEBA mixtures below).

All crosslinked materials were prepared under epoxy/amine stoichiometric conditions and cured according to the procedure described in the Experimental section. After complete curing, the structure was confirmed by FTIR. The complete disappearance of oxirane stretch band at 917 cm^{-1}, the presence of –OH vibration band at 3399 cm^{-1} and the lack of residual enthalpy by DSC suggest full crosslinking (Fig. 4). DSC experiments were performed on the mixture to evaluate the curing behavior of SDBB/DETDA and DDBB/DETDA. However, the requirement for elevated temperatures during the mixing process implies that the enthalpy values obtained *via* DSC are likely to be underestimated. As a result, these values were neither calculated nor discussed in the present study. Regarding the curing process, the onset temperature for both materials was around 100 °C, and full conversion was achieved at 220 °C with a heating rate of 10 °C min^{-1} (Fig. S7†). A residual melting can be noticed for SDBB/DETDA system compared to DDBB/DETDA as a result of incomplete mixing. Also, a distinct exothermic peak was observed for DDBB/DETDA beyond 220 °C, which can be attributed to disulfide degradation. In the second temperature ramp, the glass transition temperature (T_g) of the cured DDBB/DETDA was identified at 78 °C (Fig. 4b), which is 50 °C lower than that of SDBB/DETDA, which was at 129 °C. This result suggests that the aliphatic disulfide moiety present in DDBB tends to reduce the glass transition temperature, as previously observed in cystamine-based epoxy vitrimers.[26]

In order to investigate the dynamic properties of both materials, stress-relaxation experiments were performed at temperatures ranging from 150 °C to 180 °C and 120 °C to 160 °C for SDBB/DETDA and DDBB/DETDA, respectively. The results of normalized stress relaxation curves are presented in Fig. 5 (Fig. S8† for non-normalized version). The stress relaxation curves were fitted to a stretched exponential decay as commonly used for vitrimers.[33,34] On the basis of Kohlrausch–Williams–Watts's model (KWW)[35–37] for viscoelastic fluids, the stress relaxation behavior and the characteristic average relaxation time $\langle\tau\rangle$ of the vitrimer can be respectively calculated according to eqn (6) and (7):

$$\frac{G(t)}{G_0} = \frac{G_{res}}{G_0} + \left(1 - \frac{G_{res}}{G_0}\right) \exp^{\left(-\frac{t}{\tau^*}\right)^{\beta}} \quad (6)$$

$$\langle\tau\rangle = \frac{\tau^* \Gamma(1/\beta)}{\beta} \quad (7)$$

With (τ^*) the corresponding relaxation times, β ($0 < \beta \leq 1$) the stretching exponent that determines the shape of the stretched exponential decay and reflects the breadth of the relaxation time distribution, G_{res}/G_0 the fraction of the residual relaxation modulus and Γ the gamma function.[33,34] All fitting data are gathered in Table S1.†

A significant acceleration of the relaxation rate by a factor of about 100 is clearly visible for DDBB in comparison to SDBB (Fig. 5a and b). This difference in even more visible in Fig. 5c, where a relaxation time $\langle\tau\rangle$ of 2.9 s is extracted at 160 °C, while 237 s (≈4 min) is obtained for SDBB. This acceleration can be attributed to the presence of both disulfide and imine bonds available in the building block, allowing for a higher amount of dynamic exchanges to occur in contrast to single imine-based SDBB building block. However, the decrease of the glass transition by 50 °C should not be neglected and very likely

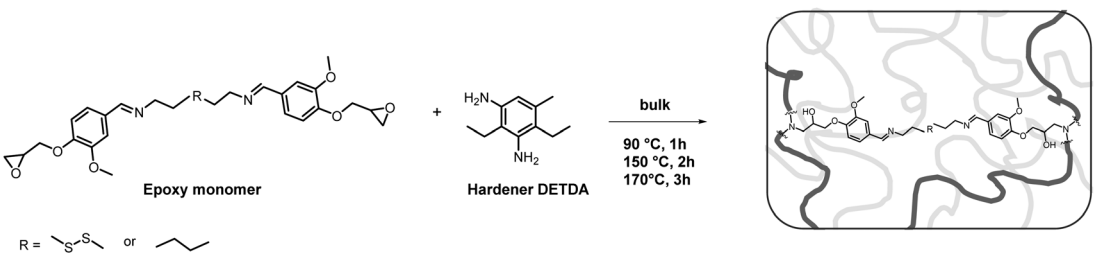

Fig. 3 Synthesis of epoxy SDBB/DETDA and DDBB/DETDA-based vitrimers.

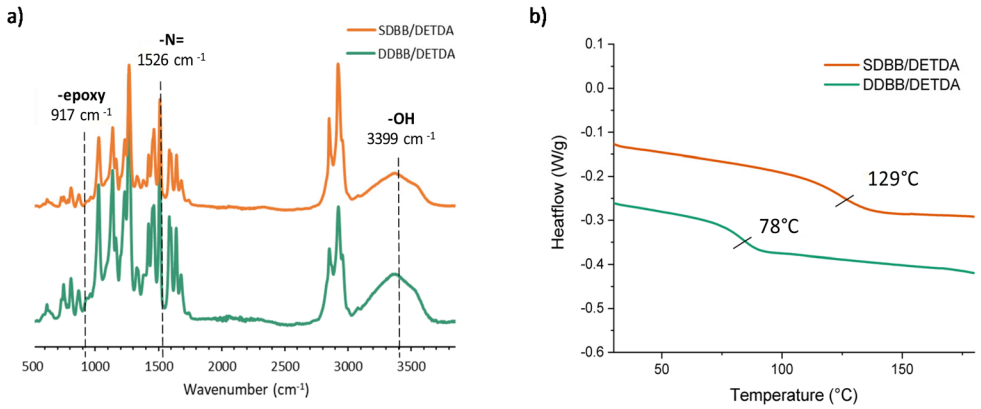

Fig. 4 (a) FTIR spectra of SDBB (orange) and DDBB (green) after curing (b) DSC thermograms of SDBB and DDBB after curing.

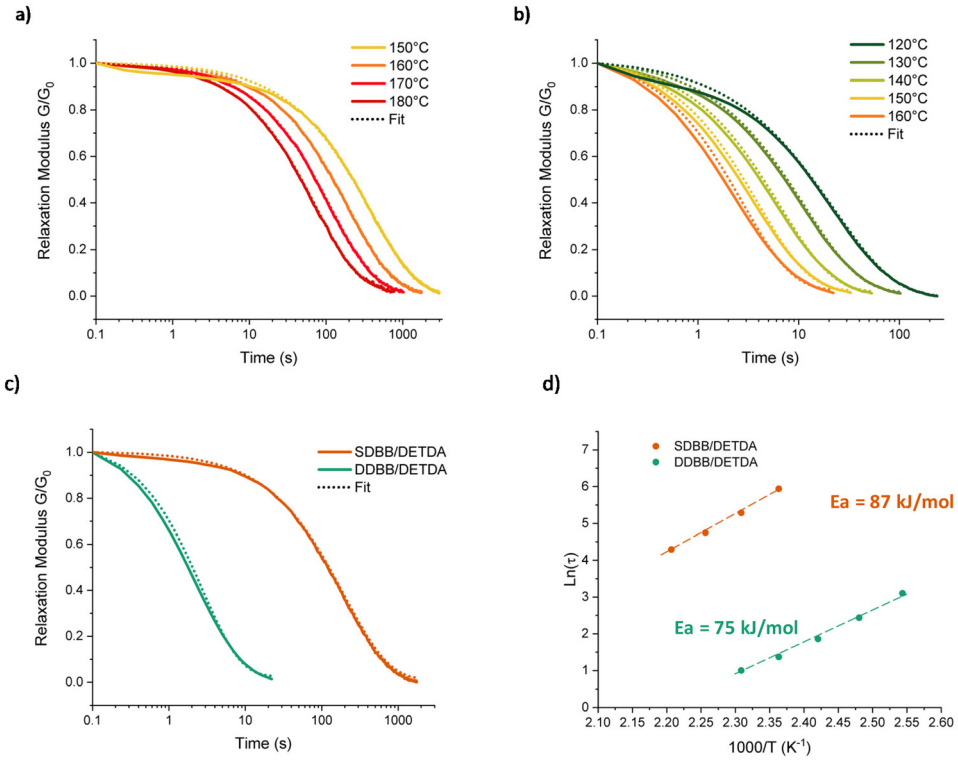

Fig. 5 Normalized stress relaxation curves of: (a) SDBB/DETDA and (b) DDBB/DETDA vitrimers (c) stress relaxation comparison of SDBB/DETDA and DDBB/DETDA at 160 °C (d) Arrhenius temperature dependence.

plays a role in the accelerated network dynamics. It is important to note that 3 s at 160 °C is one of the fastest vitrimer system ever reported, for T_g approaching 80 °C.[38] In fact, this system is even faster that our previously reported fully cystamine-based vitrimers which showed a relaxation time of 22 s at 170 °C but with a lower T_g of 53 °C.[26] This acceleration is expected to be less pronounced at higher temperature considering the difference of Arrhenius dependency. Indeed, from these relaxation times, activation energies of 75 kJ mol^{-1} and 87 kJ mol^{-1} were determined using an Arrhenius equation for DDBB/DETDA and SDBB/DETDA, respectively (see Fig. 5d and S9†).

These results suggest that the relaxation of the dual-exchange network DDBB/DETDA is less temperature-dependent than the SDBB/DETDA analogue. The faster relaxation time and the lower activation energy of the DDBB/DETDA vitrimer can be attributed to a balanced contribution of both disulfide and imine exchanges. The activation energy of 75 kJ mol^{-1} for DDBB/DETDA is located between E_a of pure imine vitrimers (SDBB, 87 kJ mol^{-1}) and pure cystamine-based vitri-

mers (57 kJ mol^{-1}).[26] Therefore, it appears that the overall macroscopic flow is dictated by both disulfide and imine exchanges, with overall an increase in concentration of dynamic groups, thereby reducing the relaxation time. This hypothesis gains support from the observed average stretching factors of 0.80 for DDBB/DETDA vitrimers, indicating a quasi-single exponential decay with homogeneous relaxation. In contrast, for SDBB/DETDA, the decay is characterized by a broader distribution with $\beta \approx 0.74$ very likely due to temperature of analyses being close to the glass transition temperature. Indeed, for both materials β is approaching 1 with increasing temperature suggesting a possible influence of T_g or low energy interactions at lower temperatures. Besides solely considering the concentration of dynamic groups, one cannot completely rule out the possible catalytic influence of imine groups on disulfide dissociation. However, this effect is challenging to evaluate and remains to be demonstrated, given the complexity of disulfide exchange, which appears to involve both radical and anionic exchanges.[39] To summarize, these results indicate that the presence of dual-dynamic covalent bonds is more efficient for the rearrangement of epoxy networks compared to single-dynamic vitrimers. However, the formulation still remains a challenge in order to efficiently use this newly formed dual-dynamic monomer into current processing techniques. Therefore, to circumvent the issue of the high melting point of DDBB and reach a better dispersion of the solid monomer, DDBB was added as building block accelerator in traditional DGEBA/4AFD-based formulations (Fig. 6). Indeed, cystamine aliphatic disulfide has recently shown a significant accelerating effect in 4AFD formulations.[26] Therefore, various proportions of DDBB such as 10, 20, and 30 w/wt% were introduced in DGEBA/4AFD formulations in order to investigate the possible accelerating effect of this dual dynamic building block.

Influence of DDBB in DGEBA/4AFD formulations

These new vitrimers were synthesized under off-stoichiometric conditions with epoxy/NH_2 = 1/1.2, as usually used in disulfide-based vitrimers[26,27,40,41] with different ratios of $DDBB_xDGEBA_y$ (with x and y standing for the mass fraction of DDBB and DGEBA, respectively, Fig. 6a) and cured according to the procedure described in the Experimental section. All formulation datas are depicted in Table 1. First, the reactivity of $DDBB_xDGEBA_y$/4AFD mixtures was analyzed by DSC (Fig. 6b).

The addition of 10 to 30 wt% of DDBB in DGEBA/4AFD formulations had different impact on both curing and resulting glass transition temperature. It only slightly reduced the T_g from the pristine DGEBA/4AFD (136 °C) down to 127 and 110 °C for 10% and 30%, respectively. It is important to note that the resulting materials still exhibited a T_g higher than 100 °C, which is a crucial criterion for composite applications. Apart from the T_g, the broadening of enthalpic peak becomes more significant as the proportion of DDBB increases. The presence of this broadening is surprising, given the structural similarity between DGEBA and DDBB. This led us to suspect the possibility of a transamination reaction occurring between the amines in 4AFD and the imine groups present in DDBB.

Such an exchange reaction would result in the release of an aliphatic amine similar to cystamine, which is known to be significantly more reactive than its aniline analogues (cystamine starts to react with DGEBA at room temperature, see Fig. S10a† for DGEBA/cystamine curing).[26] It is highly likely that this

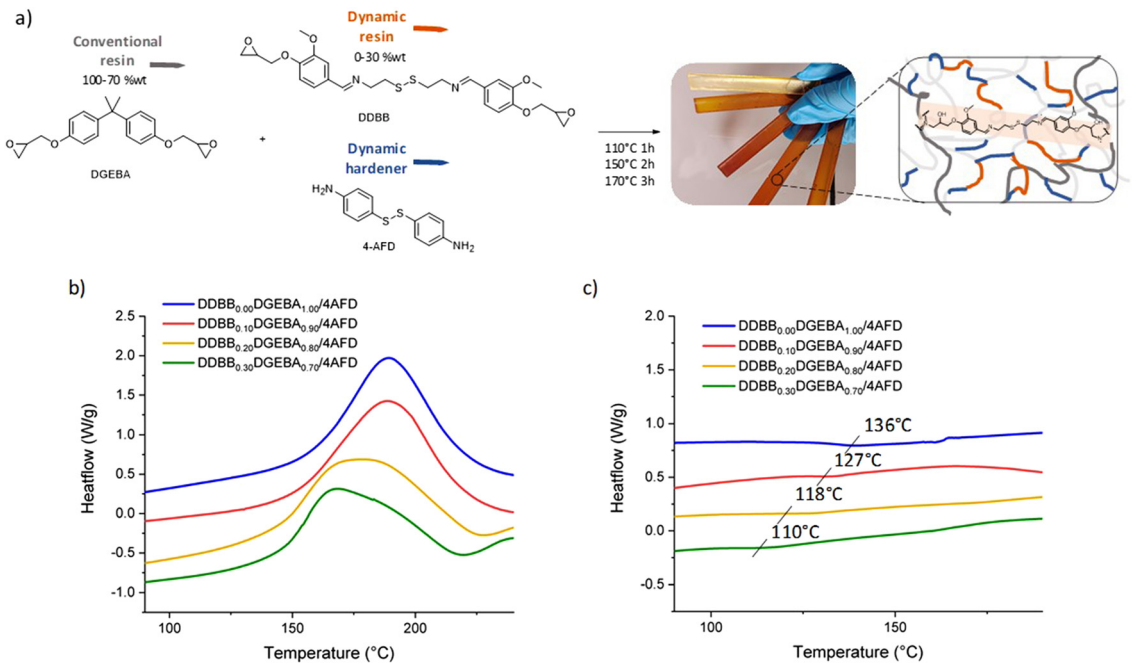

Fig. 6 (a) Synthesis of $DDBB_xDGEBA_y$/4AFD-based epoxy vitrimers (b) DSC thermograms obtained at a heating rate of 10 °C min^{-1} for $DDBB_xDGEBA_y$/4AFD mixtures (c) corresponding T_g obtained during a second heating ramp at 10 °C min^{-1}.

Table 1 Thermomechanical properties of mixtures containing various ratios of DDBB in DGEBA/4AFD formulations

Name	DDBB (wt%)	DGEBA (wt%)	Cristal-free	T_d [a] (°C)	T_g DSC[b] (°C)	E_a [d] (kJ mol^{-1})
$DDBB_{0.00}DGEBA_{1.00}$/4AFD	0	100	Yes	294	136	167[c]
$DDBB_{0.10}DGEBA_{0.90}$/4AFD	10	90	Yes	290	127	151
$DDBB_{0.20}DGEBA_{0.80}$/4AFD	20	80	Yes	286	118	136
$DDBB_{0.30}DGEBA_{0.70}$/4AFD	30	70	Yes	281	110	84

[a] T_d = 5 wt% loss. [b] T_g determined from second heating cycle of DSC. [c] Obtained from literature.[41] [d] Obtained from stress relaxation experiments.

exchange reaction occurs at temperatures below the typical reaction onset for DGEBA/4AFD at 125 °C (Fig. S10b†). This would lead to the gradual release of cystamine at the initial stage of curing, with expected immediate reactivity with epoxy at these temperatures. To evaluate this reaction, the phenolic intermediate of DDBB (Ph-DDBB) was synthetized in a view of eliminating parasite reactions between amines of 4AFD and epoxy functions of DDBB. After simple mixing at 150 °C of Ph-DDBB with 4AFD (with ratio Ph-DDBB/4AFD = 1/2.6, corresponding to $DDBB_{0.30}DGEBA_{0.70}$/4AFD formulation), the distinctive signal of the exchanged products becomes apparent (see Fig. S11†). An imine singlet is observed at 8.44 ppm, contrasting with the initial compounds that exhibited an imine signal at 8.19 ppm (Fig. S11b†). This model reaction thus confirms that this reaction very likely occurs in the curing conditions that was used for the mixture. Notably, given the reactivity initiation of aliphatic amines at room temperature, this approach facilitates a substantial shift in reactivity by approximately 75 °C.

This transamination reaction appears very common but is somehow rarely considered in various reported papers dealing with imine and epoxy.[42–44] This reaction is not necessarily prejudicial neither with regards to materials nor dynamic properties, but this could have an impact in the fundamental understanding of the material properties. Most of the time, this reaction is not considered because the building block used for preparing the imine and the crosslinker show similar structures.[23]

In addition to the model reaction, we evaluated the thermal stability of DDBB resin without a hardener using DSC and FTIR (refer to Fig. S3–S4†). During the first heating cycle, we observed two enthalpic signals at 210 °C and 240 °C. A visible T_g was determined at 93 °C during the second heating cycle. These results suggest that DDBB can self-initiate epoxy ring-opening polymerization at relatively high temperatures and that, at around 240 °C, the disulfide linkages appear to degrade. To go further into this investigation, FTIR spectra were recorded on DDBB before curing and DDBB after curing for 180 min at 150 °C and 120 min at 170 °C. We are able to observe the emergence of signals at 3401 cm^{-1}, corresponding to hydroxyl groups and signal at 2000–2200 cm^{-1} that could be attributed to thiol signals. Moreover, the oxirane signal around 909 cm^{-1} disappeared after curing (Fig. S4†). From these results, we can safely assume that DDBB is not thermally stable at temperatures beyond 200 °C and that epoxy ring-opening polymerization occurred. Nonetheless, this doesn't seem to have neither an influence on crosslinking efficiency and kinetics nor on mechanical properties of cured materials as the curing is conducted at 150 °C. Similar behavior is also observed on SDBB, as expected although the second enthalpic peak attributed to disulfide degradation is not observed (Fig. S5†).

Thermogravimetric analysis at 5 wt% loss on cured materials showed that all resins have comparable degradation temperature and do not degrade up to 280 °C, as showed in Fig. S12b.† Nonetheless, a gradual decrease of T_d is observed with the increasing amount of DDBB into the formulations. This effect can be ascribed to the presence of the less energetically stable aliphatic cystamine bonds into DDBB compared to the 100% DGEBA reference.[41] These results confirm that adding small amount of DDBB to DGEBA/4AFD material does not have a pronounced influence on the thermal behavior of the materials. However, according to our expectations, the proportion of DDBB could have considerable influence over dynamic properties. This effect over dynamic exchanges is more deeply investigated and discussed in the next section.

All mixtures were studied *via* stress relaxation experiments at different temperatures. All rheological results, at each temperature from 170 °C to 200 °C, are reported in Fig. S13 and Table S3.† Fig. 7a shows the stress relaxation of the different vitrimers with various weight fractions of DDBB at 190 °C. These stress relaxation curves reveal that these $DDBB_xDGEBA_y$/4AFD vitrimers can completely relax the stress with G_{res}/G_0 approaching zero for all formulations, except for non-doped reference material DGEBA/4AFD which did not reach a complete relaxation under the same conditions. These results highlight the accelerated exchanges for formulations with the addition of DDBB. As a basis for comparison, the average relaxation time at 190 °C of $DDBB_{0.30}DGEBA_{0.70}$/4AFD was 21 s *versus* 25 min for DGEBA/4AFD.

A good fit was obtained for both materials with R^2 of 0.99 for all relaxation curves. Average β values in the range of 0.47 for $DDBB_{0.10}DGEBA_{0.90}$/4AFD and 0.63 for $DDBB_{0.30}DGEBA_{0.70}$/4AFD were obtained indicating a broader distribution of relaxation times for the network containing 10 wt% compared to 30 wt% material. This result is rather unexpected as heterogeneity would have been more expected with increasing amount of DDBB. However, these beta values tend to rise with increasing temperature (about 0.60), again suggesting a possible influence of the T_g on the β coefficient. Indeed, the three materials showed different glass transitions but all stress relaxation experiments were conducted at the same temperature. Therefore, the influence of T_g is unequal for all formulations.

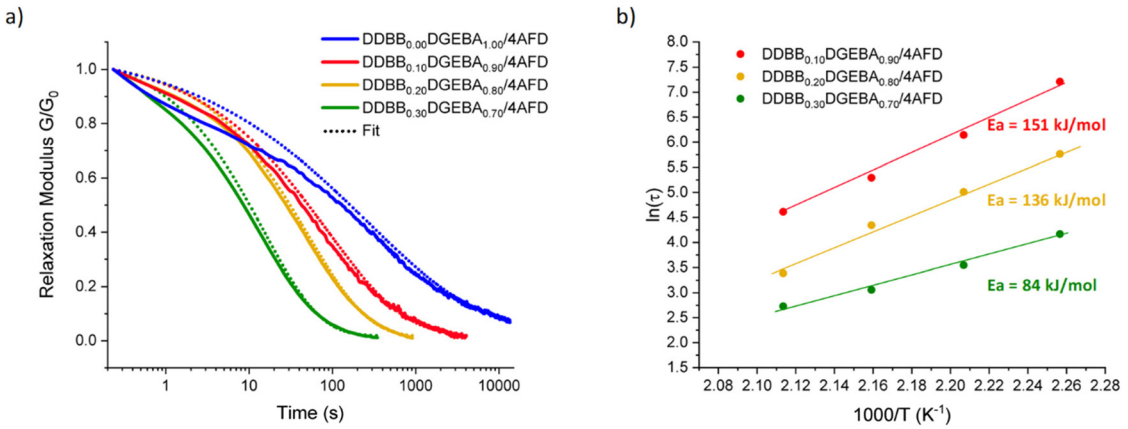

Fig. 7 (a) Stress relaxation experiments at 190 °C of $DDBB_xDGEBA_y$/4AFD formulations with *x* ranging from 0 to 0.30 and *y* from 1.00 to 0.70 and (b) corresponding Arrhenius dependence.

From the extracted relaxation times, the corresponding viscous flow E_a was calculated from the slope through linear regression (Fig. 7b), and apparent E_a values of 84, 136 and 151 kJ mol^{-1} have been determined for $DDBB_{0.30}DGEBA_{0.70}$/4AFD, $DDBB_{0.20}DGEBA_{0.80}$/4AFD and $DDBB_{0.10}DGEBA_{0.90}$/4AFD, respectively (Table 1). It is interesting to note that a 30 w/w% of DDBB significantly reduces the activation energy of pure DGEBA/4AFD from 167 kJ mol^{-1} to 84 kJ mol^{-1}. This value is remarkably close to the activation energy of pure DDBB/DETDA, which is 75 kJ mol^{-1}.

Swelling experiments were also performed in order to assess the network integrity of the vitrimer materials. The materials were immersed in various organic solvents ($CHCl_3$, DMF, DMSO, THF) and the swelling ratio and soluble fraction were calculated (Table S4†). The soluble fractions were found to be below 5% for all solvents, with an even lower soluble fraction observed for DDBB-containing formulations. This suggests that the DDBB building block has no discernible influence on the network integrity. However, a higher swelling ratio was noticed with increasing concentration of DDBB, likely due to reduced crosslink density and changes in polarity.

Finally, the reprocessability of synthesized vitrimer materials were evaluated through compression molding experi-

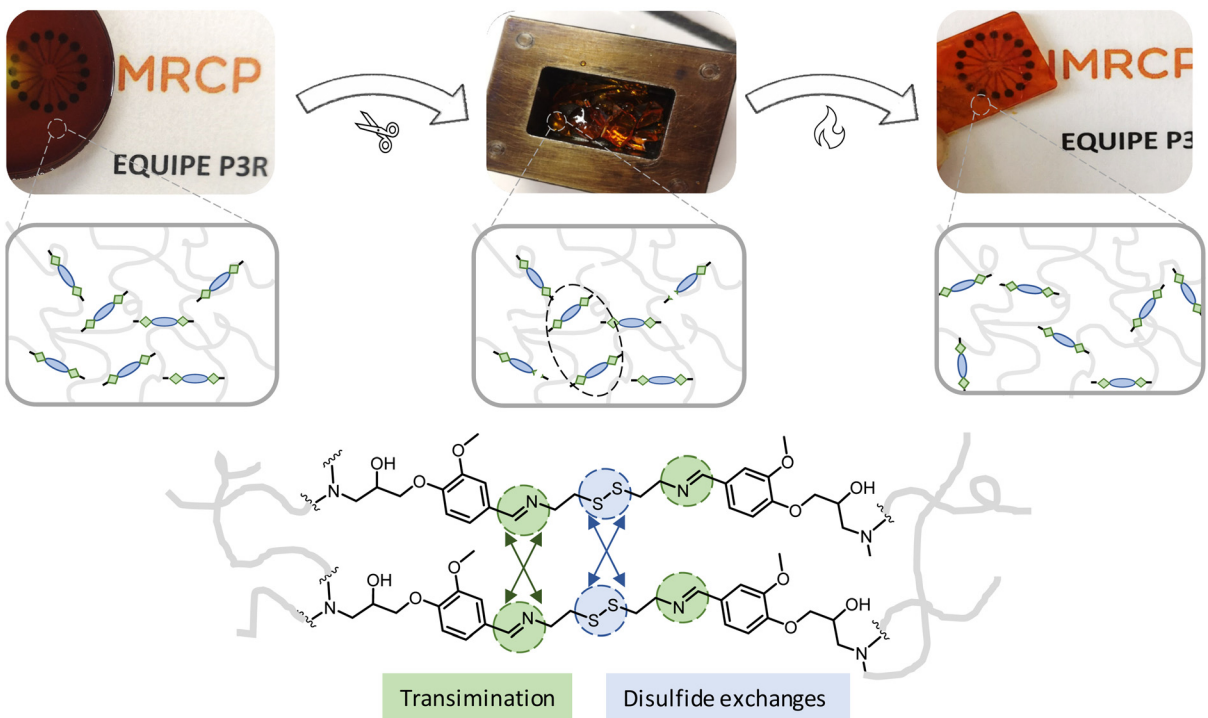

Fig. 8 Example of reprocessing experiment *via* compression moulding of $DDBB_{0.30}DGEBA_{0.70}$/4AFD formulation in a hot press at 170 °C.

ments. $DDBB_{0.30}DGEBA_{0.70}$/4AFD was broken into small pieces and was fully reshaped into rectangular specimens under hot press at 170 °C for 35 min, (Fig. 8). These new epoxy vitrimers doped with DDBB showed reprocessing properties much faster than the conventional material DGEBA/4AFD that needed more than 240 min to be partially recovered under hot press. After reprocessing, similar T_g and relaxation times were observed suggesting efficient property recovery (Fig. S14†).

Conclusion

In conclusion, this study introduces a new symmetrical and partially biosourced DDBB epoxy building block, for the preparation of epoxy/amine vitrimers with enhanced relaxation properties. A comprehensive comparison of its dynamic properties with a single-based imine-based epoxy analogue (SDBB) revealed a substantial acceleration in the relaxation rate, approximately 100 times faster. The accelerated relaxation time and lower activation energy in DDBB vitrimers result from a balanced contribution of both disulfide and imine exchanges, positioning it between pure imine and pure aliphatic disulfide-based vitrimers. Then, to address the high melting point of DDBB and improve monomer formulation, DDBB was introduced as a building block accelerator in traditional epoxy/disulfide DGEBA/4AFD vitrimer formulations. Various proportions of DDBB (10, 20, and 30 w/wt%) were incorporated, with an important accelerating effect noticed, particularly in comparison to standard DGEBA/4AFD formulation. Although a broader reactivity was evidenced as a result of exchange between the imines of DDBB and amines of 4AFD while curing. The reported materials exhibited full and fast stress relaxations (21 s for $DDBB_{0.30}DGEBA_{0.70}$/4AFD), much faster than relaxation rate of classical DGEBA/4AFD (25 min). Importantly, this acceleration did not significantly impair the performances of the materials with still competitive T_g values in the range of 120 °C. These findings open possibilities to further optimize and tune vitrimer dynamics with dual-dynamic monomers for disulfide-based vitrimer formulations.

Author contributions

All authors have given approval to the final version of the manuscript.

Conflicts of interest

The authors declare no competing financial and scientific interests.

Acknowledgements

This work was supported by the VIBES project. This project has received funding from the Bio-Based Industries Joint Undertaking (JU) under grant agreement no. 101023190. The JU receives support from the European Union's Horizon 2020 Research and Innovation Program and the Bio-Based Industries Consortium. This article reflects only the authors' view, and the JU is not responsible for any use that may be made of the information it contains.

References

1 S. Ma and D. C. Webster, *Prog. Polym. Sci.*, 2018, **76**, 65–110.
2 R. Auvergne, S. Caillol, G. David, B. Boutevin and J.-P. Pascault, *Chem. Rev.*, 2014, **114**, 1082–1115.
3 S. Wang, S. Ma, C. Xu, Y. Liu, J. Dai, Z. Wang, X. Liu, J. Chen, X. Shen, J. Wei and J. Zhu, *Macromolecules*, 2017, **50**, 1892–1901.
4 S. Ma, D. C. Webster and F. Jabeen, *Macromolecules*, 2016, **49**, 3780–3788.
5 S. Ma, X. Liu, Y. Jiang, Z. Tang, C. Zhang and J. Zhu, *Green Chem.*, 2013, **15**, 245–254.
6 E. D. Hernandez, A. W. Bassett, J. M. Sadler, J. J. La Scala and J. F. Stanzione, *ACS Sustainable Chem. Eng.*, 2016, **4**, 4328–4339.
7 J. Wan, J. Zhao, B. Gan, C. Li, J. Molina-Aldareguia, Y. Zhao, Y.-T. Pan and D.-Y. Wang, *ACS Sustainable Chem. Eng.*, 2016, **4**, 2869–2880.
8 N. Mattar, A. R. De Anda, H. Vahabi, E. Renard and V. Langlois, *ACS Sustainable Chem. Eng.*, 2020, **8**, 13064–13075.
9 N. J. Van Zee and R. Nicolaÿ, *Prog. Polym. Sci.*, 2020, **104**, 101233.
10 W. Denissen, J. M. Winne and F. E. Du Prez, *Chem. Sci.*, 2016, **7**, 30–38.
11 J. Zheng, Z. M. Png, S. H. Ng, G. X. Tham, E. Ye, S. S. Goh, X. J. Loh and Z. Li, *Mater. Today*, 2021, **51**, 586–625.
12 M. Guerre, C. Taplan, J. M. Winne and F. E. Du Prez, *Chem. Sci.*, 2020, **11**, 4855–4870.
13 A. Ruiz de Luzuriaga, R. Martin, N. Markaide, A. Rekondo, G. Cabañero, J. Rodríguez and I. Odriozola, *Mater. Horiz.*, 2016, **3**, 241–247.
14 I. Azcune and I. Odriozola, *Eur. Polym. J.*, 2016, **84**, 147–160.
15 L. Li, X. Chen and J. M. Torkelson, *ACS Appl. Polym. Mater.*, 2020, **2**(11), 4658–4665.
16 V. Schenk, R. D'Elia, P. Olivier, K. Labastie, M. Destarac and M. Guerre, *ACS Appl. Mater. Interfaces*, 2023, **15**, 46357–46367.
17 D. Sanchez-Rodriguez, S. Zaidi, Y. Jahani, A. Ruiz de Luzuriaga, A. Rekondo, P. Maimi, J. Farjas and J. Costa, *Polym. Degrad. Stab.*, 2023, **217**, 110543.
18 M. Chen, L. Zhou, Y. Wu, X. Zhao and Y. Zhang, *ACS Macro Lett.*, 2019, **8**, 255–260.
19 O. Konuray, S. Moradi, A. Roig, X. Fernández-Francos and X. Ramis, *ACS Appl. Polym. Mater.*, 2023, **5**, 1651–1656.

20 H. Liu, Z. Sun, L. Wei, Y. Liu, S. Zhou, Q. Ge, C. Liu and X. Li, *Polym. Test.*, 2023, **126**, 108145.
21 D. J. Fortman, R. L. Snyder, D. T. Sheppard and W. R. Dichtel, *ACS Macro Lett.*, 2018, **7**, 1226–1231.
22 S. Xiang, L. Zhou, R. Chen, K. Zhang and M. Chen, *Macromolecules*, 2022, **55**, 10276–10284.
23 C. Luo, W. Wang, W. Yang, X. Liu, J. Lin, L. Zhang and S. He, *ACS Sustainable Chem. Eng.*, 2023, **11**, 14591–14600.
24 X. Xu, S. Ma, H. Feng, J. Qiu, S. Wang, Z. Yu and J. Zhu, *Polym. Chem.*, 2021, **12**, 5217–5228.
25 Y. Hao, L. Zhong, T. Li, J. Zhang and D. Zhang, *ACS Sustainable Chem. Eng.*, 2023, **11**, 11077–11087.
26 S. Guggari, F. Magliozzi, S. Malburet, A. Graillot, M. Destarac and M. Guerre, *ACS Sustainable Chem. Eng.*, 2023, **11**, 6021–6031.
27 A. Genua, S. Montes, I. Azcune, A. Rekondo, S. Malburet, B. Daydé-Cazals and A. Graillot, *Polymers*, 2020, **12**, 2645.
28 A. Llevot, E. Grau, S. Carlotti, S. Grelier and H. Cramail, *Macromol. Rapid Commun.*, 2016, **37**, 9–28.
29 M. Fache, A. Viola, R. Auvergne, B. Boutevin and S. Caillol, *Eur. Polym. J.*, 2015, **68**, 526–535.
30 M. Fache, B. Boutevin and S. Caillol, *ACS Sustainable Chem. Eng.*, 2016, **4**, 35–46.
31 M. A. Rashid, M. N. Hasan, M. A. R. Dayan, M. S. Ibna Jamal and M. K. Patoary, *Reactions*, 2023, **4**, 66–91.
32 J. M. Matxain, J. M. Asua and F. Ruipérez, *Phys. Chem. Chem. Phys.*, 2016, **18**, 1758–1770.
33 L. Li, X. Chen, K. Jin and J. M. Torkelson, *Macromolecules*, 2018, **51**, 5537–5546.
34 A. Dhinojwala, J. C. Hooker and J. M. Torkelson, *J. Non-Cryst. Solids*, 1994, **172–174**, 286–296.
35 K. S. Fancey, *J. Mater. Sci.*, 2005, **40**, 4827–4831.
36 J. D. Ferry, *Viscoelastic Properties of Polymers*, John Wiley & Sons, 1980.
37 G. Williams and D. C. Watts, *Trans. Faraday Soc.*, 1970, **66**, 80.
38 C. Taplan, M. Guerre, J. M. Winne and F. E. Du Prez, *Mater. Horiz.*, 2020, **7**, 104–110.
39 S. Nevejans, N. Ballard, J. I. Miranda, B. Reck and J. M. Asua, *Phys. Chem. Chem. Phys.*, 2016, **18**, 27577–27583.
40 I. Azcune, A. Huegun, A. Ruiz de Luzuriaga, E. Saiz and A. Rekondo, *Eur. Polym. J.*, 2021, **148**, 110362.
41 A. Ruiz de Luzuriaga, G. Solera, I. Azcarate-Ascasua, V. Boucher, H.-J. Grande and A. Rekondo, *Polymer*, 2022, **239**, 124457.
42 X.-M. Ding, L. Chen, Y.-J. Xu, X.-H. Shi, X. Luo, X. Song and Y.-Z. Wang, *ACS Sustainable Chem. Eng.*, 2023, **11**, 14445–14456.
43 Z. Miao, C. Peng, L. Xia, H. Xu, S. He, C. Chi, J. Zhong, S. Wang, W. Luo, G. Chen, B. Zeng and L. Dai, *ACS Appl. Polym. Mater.*, 2023, **5**, 6325–6337.
44 A. Roig, P. Hidalgo, X. Ramis, S. De la Flor and À. Serra, *ACS Appl. Polym. Mater.*, 2022, **4**, 9341–9350.